Journal of Pain Research

Dovepress
Taylor & Francis Group

Open Access Full Text Article

ORIGINAL RESEARCH

Efficacy and Potential Mechanisms of Yi-Ping Lin Circum-Knee Acupuncture in the Treatment of Knee Osteoarthritis

Lijun Huang[1], Xingyou Deng[1], Yanling Jin[1], Jing Li[1], Xiangnong Wu[1], Youlong Xiong[1], Shaofeng Guo[2], Shaoyue Yan[3], Shengdi Lu[1], Dajun Chen[4]

[1]Yunnan Provincial Hospital of Traditional Chinese Medicine, Kunming, Yunnan, People's Republic of China; [2]Yiliang County North Ancient Town Central Hospital, Kunming, Yunnan, People's Republic of China; [3]Ma Zhan Township Health Center, Tengchong, Yunnan, People's Republic of China; [4]Yanshan County Hospital of Traditional Chinese Medicine Benge Branch, Yunnan, People's Republic of China

Correspondence: Xingyou Deng, Yunnan Provincial Hospital of Traditional Chinese Medicine, Kunming, Yunnan, 650051, People's Republic of China, Email 417772851@qq.com

Background: Degenerative knee osteoarthritis (KOA) may lead to disability in adults. Current treatment modalities for KOA often involve significant side effects and high costs. Yi-Ping Lin Circum-knee Acupuncture (CKA-L) emerged as a cost-effective and nearly side-effect-free alternative. However, its efficacy and the underlying mechanisms remain unclear, which raised our concern.

Methods: Female SD rats were randomly divided into 4 groups: Sham, Model, CKA-L treatment (Treatment), and positive control (Piroxicam). The Arthritis Index (AI) and body weights were recorded. ELISA was used to quantify levels of IL-1β and TNF-α. X-ray, HE, and Toluidine blue staining were employed to assess cartilage regeneration. Transcriptome sequencing was performed to identify differentially expressed genes (DEGs). Bioinformatics methods were employed to perform functional enrichment and protein-protein interaction (PPI) analysis on these DEGs. RT-qPCR and Western blot were utilized to determine the hub genes.

Results: Both CKA-L and piroxicam effectively alleviated KOA, albeit with slower response times for CKA-L (4 weeks in CKA-L group vs 3 weeks in piroxicam group). ELISA results demonstrated significant reductions in pro-inflammatory cytokines, with a pronounced decline in TNF-α in the Treatment group ($p< 0.01$). CKA-L markedly increased chondrocyte populations and narrowed the knee joint gap. Transcriptome analysis identified 3363 DEGs. Functional enrichment analyses highlighted significant associations with DNA repair, inhibition of cysteine-type endopeptidases, and cell-cycle regulation. The PPI analysis of DEGs designated five hub genes: Bgn, Ctsb, Lum, Serpine1, and Tnfaip6, which demonstrated consistent transcriptional and translational expression levels.

Conclusion: CKA-L promotes chondrocyte proliferation and provides effective treatment for KOA, with the advantages of low price, low side effects, and convenient operation.

Keywords: degenerative knee osteoarthritis, acupuncture, transcriptome sequencing, Osteoarthritis, traditional Chinese medicine

Introduction

Osteoarthritis (OA) is an inflammatory disease caused by abnormalities of the joints or periarticular tissues.[1] It is a panarticular disease affecting all joint tissues, including changes in the synovium and infrapatellar fat pad.[2] Notably, the inflammatory response originates not only from the articular cartilage itself, but more critically from immune-inflammatory abnormalities in the periarticular tissues—particularly structures such as the synovium, subchondral bone, and infrapatellar fat pad.[3] By 2050, experts predict that OA prevalence may soar to one billion cases globally.[4] The knee joint consists of the femur, tibia, and fibula, and its inflammation is a common one in OA. Knee osteoarthritis (KOA), also known as degenerative KOA or hypertrophic arthritis of the knee, involves damage to the articular cartilage, meniscus, and ligaments. Moreover, irregularities in the knee joint can cause undue medial or lateral loading on the tibial and femoral components.[5] The exact cause of KOA remains unknown. However, factors like natural aging and trauma are suspected contributors.[6] Certainly, factors such as obesity, aging, and gender should not be overlooked.[7–9] Moreover,

Received: 4 July 2025
Accepted: 21 October 2025
Published: 7 November 2025

in the United States, approximately 2% of individuals over 17 and 10% of those aged 65 and older are affected by KOA.[6] Treatments for KOA typically fall into two main categories: non-surgical and surgical interventions. Non-surgical approaches prioritize weight loss,[10] physical activity,[11,12] and pharmacotherapy. Notably, non-steroidal anti-inflammatory drugs (NSAIDs) are frequently used such as piroxicam.[13] Although injection alternatives may mitigate side effects, long-term NSAID usage still poses risks to the liver, kidneys, and gastrointestinal tract.[14,15] Short-term or intermittent use of acetaminophen and corticosteroid injections are also commonly used treatments. However, these treatments carry the risk of hepatotoxicity and may elevate the likelihood of cartilage deterioration, and treatment is expensive.[16,17] In surgical treatment, arthroscopy is recommended due to its favorable efficacy.[18,19] However, some studies also indicate that the benefits of arthroscopy may be short-term or effective only for certain specific groups of patients with KOA.[20,21] Despite the variety of KOA treatments available, these disadvantages mentioned above underline the urgent need for new therapies that are more universally effective and exhibit fewer side effects.

Lifetime medical expenses linked to KOA in US adults total approximately $12,400.[22] In contrast, the average cost for acupuncture treatment is merely ¥19.32 (Approximately 0.027 US dollars).[23,24] This indicates that acupuncture can significantly reduce healthcare expenses. Research highlights acupuncture's considerable efficacy for OA when compared to other forms of traditional Chinese medicine (TCM), showing minimal side effects.[25] Such benefits enhance acupuncture's prominence in therapeutic contexts. Acupuncture operates on the meridian theory intrinsic to Chinese medicine, historically utilized for thousands of years to alleviate various ailments by activating specific body surface points (acupoints) and promoting self-regulatory functions.[26] Current evaluations indicate acupuncture effectively addresses 81 medical conditions via efficacy grading and 68 via evidence-based analysis, predominantly in pain, neurological, and immunoendocrine disorders.[27] As a long-established TCM technique, acupuncture is widely applied in the treatment of KOA.[28–30] The primary variations in acupuncture methods stem from the selection of acupoints and the techniques employed. Commonly chosen acupoints in clinical practice for KOA include local points such as Xuehai, Yinlingquan, Yanglingquan, Xiyang, Zusanli, and Heding.[28,31–33] Additionally, practitioners may utilize acupoints derived from clinical experiences, such as Guan's Six Spirit points for knee pain.[34] Frequently utilized acupuncture methods encompass traditional needling, moxibustion, and warming acupuncture. Innovations that integrate modern scientific technology for acupuncture, such as electroacupuncture.[28] Occasionally, practitioners may employ a combination of techniques for treatment.[35] Furthermore, acupuncture serves as an adjunctive treatment modality for KOA, enhancing the overall therapeutic efficacy as reported in various studies.[36,37] Yi-Ping Lin Circum-knee Acupuncture (CKA-L) is an acupuncture technique developed for knee arthritis pain based on traditional acupuncture combined with the Three-Level Pattern Identification Framework (Disease Identification, Meridian-Based Pattern Identification, and Symptom-and-Sign Pattern Identification). In previous clinical studies, we found CKA-L to be significantly effective for knee arthritis pain (p=0.024).[38] Nevertheless, the scarcity of robust research hinders the broader acceptance of acupuncture.

This study set out to apply a new acupuncture technique, CKA-L, to treat KOA. Four groups were set up: Sham group, KOA model group, CKA-L treatment group, and piroxicam treatment group to compare and analyze the treatment effect of CKA-L on KOA. Our research may offer a cost-effective approach for KOA therapy, with minimal adverse effects. It also provides a scientific basis for the treatment of KOA with CKA-L and contributes to the evidence-based medicine of acupuncture.

Methods

Degenerative Knee Osteoarthritis Model

Female Sprague-Dawley (SD) rats (160~220 g, 6~8 weeks) were purchased from the Experimental Animal Center of Kunming Medical University (License No. SCXK (Dian) 2020-0004). SD rats were housed at a temperature of 22 ± 1 °C. All animals were anesthetized by intraperitoneal injection of Ketamine & xylazine at a dose of 100 mg/kg and 5 mg/kg. The skin at the knee joint was incised in the Sham group and sutured as soon as it was exposed. The model was constructed for 4 weeks and then consecutively treated with CKA-L or piroxicam for 4 weeks to form the Treatment and Piroxicam groups, respectively. CKA-L treatment was required 3 times a week. The piroxicam was administered to rats by gavage at a dose of 12 mg/kg once daily. The methods of model construction[39] were as follows: after anesthesia, SD

rats were fixed in the supine position, the hair at the surgical site was removed and disinfected, and the skin of the medial tibia was incised centered on the horizontal plane of the tibial plateau of the knee joint, the medial collateral ligament was exposed, and it was carefully severed. Then, the knee joint cavity was opened horizontally, the medial meniscus was carefully dissected from the middle position, and the anterior cruciate ligament was dissected deep in the joint cavity. Finally, the joint cavity was closed, and sutured, and the appropriate amount of penicillin powder was sprinkled on the surgical site to fight infection. Female SD rats were randomly divided into four groups (n=3): the Sham group, the Model group, the CKA-L treatment group (Treatment), and the Piroxicam tablets (a positive drug for KOA) treatment group (Piroxicam). Euthanasia of SD rats with cervical dislocation after anesthesia with sodium pentobarbital (120 mg/kg) after completing the treatment experiment. All animal experiments conducted in this study were approved by the Experimental Animal Ethics Committee of Yunnan Provincial Hospital of Traditional Chinese Medicine (Ethics Approval No.: DSL-2024-048) and strictly adhered to the relevant provisions of the "Guidelines for Ethical Review of Laboratory Animal Welfare" (GB/T 35892-2018), ensuring the welfare of experimental animals was fully safeguarded.

Yi-Ping Lin Circum-Knee Acupuncture Treatment Methods and Prognostic Assessment

CKA-L treatments focused on specific acupoints, including the inner and outer Xiyan, Heding, and weizhong acupoints. Acupuncture points are localized according to relevant standards.[40] The Xiyan acupoints, located beside the patellar ligament when the knee is flexed, consist of the inner and outer Xiyan. The Heding acupoint lies at the patellar apex (the depression above the midpoint of the patellar base). The weizhong acupoint resides at the center of the posterior knee depression, aligned with the popliteal transverse stripe (Figure 1A). During treatment, rats were administered inhalation anesthesia with 1% isoflurane in 100% O_2, at a flow rate of 1–2 L/min, a stable respiratory rate of rats at 50–70 breaths/min to ensure animal compliance. The needles employed measured 25×25 mm, utilizing both flat tonic and flat diarrhea techniques. Specifically, needles were gently inserted 3–5 mm into the Xiyan and Heding acupoints, and 5–7 mm into the weizhong acupoint. Each needle was rotated gently at each acupoint for 30 seconds and then left in place for 30 min before careful withdrawal. To monitor progress, rats were weighed every three days, and a 4-point arthritis index (AI) score[41] was introduced to assess the severity of KOA, as detailed in Table 1. Additionally, X-ray (Portable X-ray Diagnostic System for Animals, HF100Ha, Hitachi, Japan) imaging was used to evaluate the treatment efficacy.

ELISA

To collect synovial fluid for ELISA, a 1 mL syringe aspirated 0.2 mL of distilled water and transferred it into the joint cavity for repeated aspiration. Synovial fluid is a viscous liquid secreted by synovial cells, rich in hyaluronic acid, lubricin, and plasma filtrate components. Its primary functions include lubricating articular cartilage, reducing friction, nourishing cartilage, and cushioning mechanical impacts. Within an inflammatory microenvironment, synovial fluid releases inflammatory mediators that induce catabolic processes in chondrocytes, accelerating degradation of the cartilage matrix.[42] This procedure adhered to the guidelines provided by the Cytokine IL-1β (E-EL-R0012c) and TNF-α (E-EL-R2856c) kits (Elabscience, China). Optical density values for each well were measured using an enzyme labeling instrument (ELx800, BIO-TEK, USA) at 450 nm within 15 minutes post-reaction.

Decalcification and Tissue Staining Analysis

Whole knee joints of rats were taken and fixed in 4% frozen paraformaldehyde and then immersed in 5% EDTA for decalcification. Cartilage slices were dehydrated and embedded in paraffin. Consecutive 5 μm sections were made with a paraffin slicer (Leica, Germany).

HE Staining: tissue sections underwent staining with hematoxylin for 5 minutes. They were then immersed in a hematoxylin differentiation solution for 30 seconds and were washed with running water. Subsequently, sections received eosin staining for 1 to 2 minutes before dehydration and sealing for holographic scanning.

Toluidine Blue Staining: dried at 60 °C for at least 30 min and rehydrated with xylene and graded alcohol. Samples were immersed in a toluidine blue staining solution for 3 min and then rinsed with distilled water. Sections were

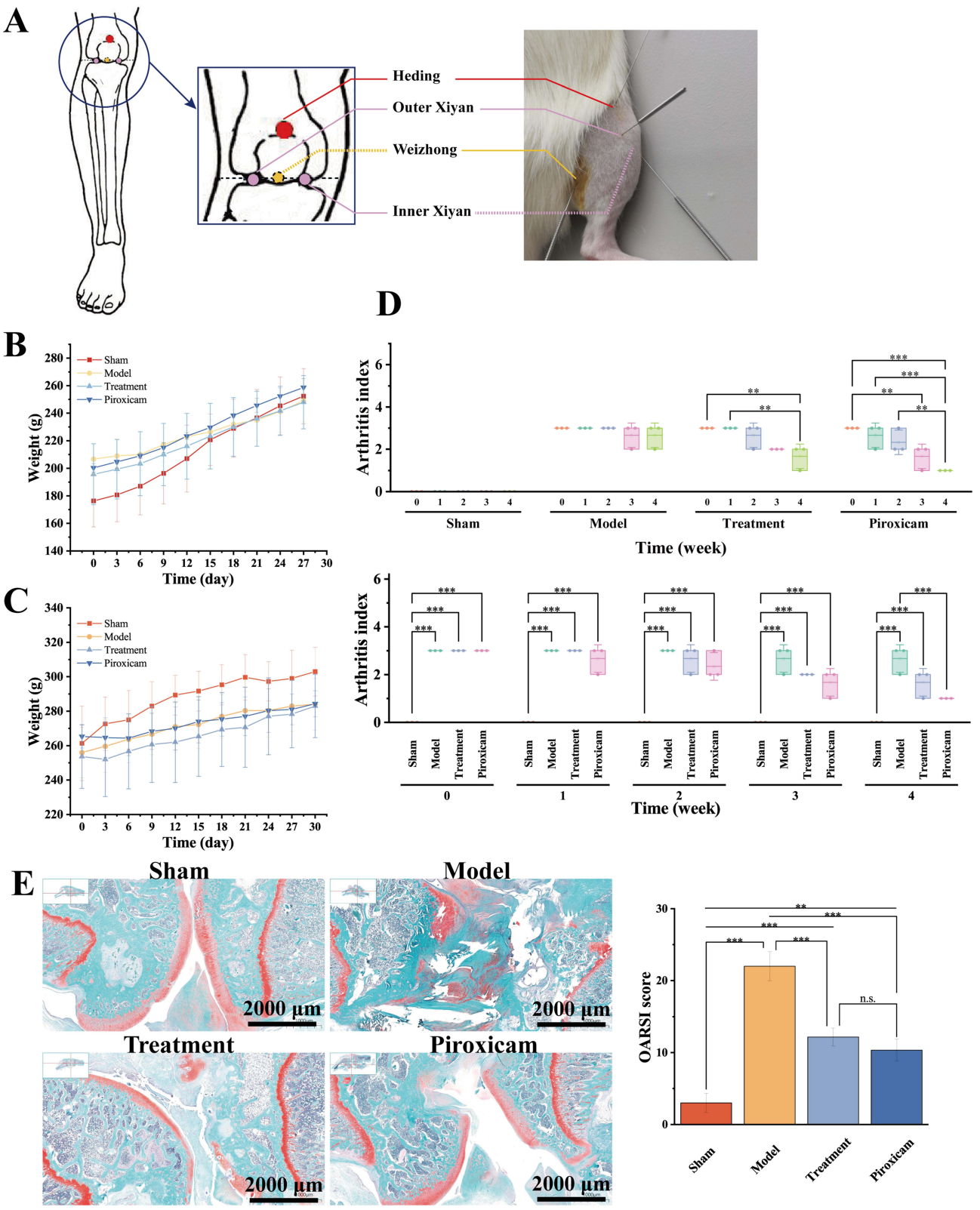

Figure 1 CKA-L effectively treats degenerative knee osteoarthritis. (**A**) Schematic diagram of CKA-L treatment acupoints. The red one is Heding, the two purple ones are the Inner and Outer Xiyan, and the yellow one is Weizhong. The dotted line indicates behind. (**B** and **C**) Body weight assessment of rats at 4 weeks after modeling (**B**) and 4 weeks during treatment (**C**). (**D**) Comparison of arthritis index within (upside) and between (downside) groups during treatment. (**E**) Knee joint damage was evaluated using safranin O-fast green staining and scored according to the OARSI grading system. Data are expressed as mean ± SD of four parallel independent experiments. Statistical significance was indicated as ** $p \leq 0.01$, *** $p \leq 0.001$.

Table 1 Arthritis Index

Symptomatic	Mark
No arthritis	0
Joints appear slightly swollen or with red spots	1
Joints show moderate swelling or redness	2
Joints show signs of severe redness and swelling	3
Severe swelling or redness of the joints and inability to walk with weight-bearing	4

differentiated in 95% ethanol for a few seconds to 1 min followed by anhydrous ethanol for rapid dehydration. Xylene was transparent and slices were sealed with neutral gum for holographic scanning.

Safranin O-Fast Green staining: The samples were dried at 60 °C for at least 30 min, then rehydrated using xylene and graded ethanol. The sections were stained with Weigert's iron hematoxylin solution for 5 min, followed by differentiation in acid ethanol for 5s and rinsing. The slices were then immersed in Fast Green solution for 30 min, washed again, and air-dried. Subsequently, the sections were stained with Safranin O solution for 1 min, and excess stain was removed with absolute ethanol. Then, the sections were cleared with xylene and mounted with neutral balsam. Finally, whole-slide images were acquired using a holographic scanning microscope.

Transcriptome Analysis

RNA sequencing was conducted on the Sham, Model, and Treatment groups (n=4). Total RNA from the samples was extracted by the TRIzol method and evaluated for quality. Library construction and sequencing were done by Novogene (Beijing, China). The samples were sequenced on the Illumina platform. Subsequently, quality control was performed on the raw data to remove low-quality reads and obtain high-quality clean data. HISAT2 (v2.0.5) was used to map the clean reads to the reference genome, with overall mapping rates ranging from 95.36% to 97.07% across all samples. Gene expression levels were quantified using the FPKM method. The results obtained were analyzed using the DESeq2 package in R.[43] Differences were screened for $|\log_2(\text{Fold Change})| \geq 1$ and $p\text{adj} \leq 0.05$ (FDR (Benjamini-Hochberg) $\leq$ 0.05). After obtaining the differentially expressed genes (DEGs), clusterProfiler software was used to perform Gene Ontology (GO)[44] and Kyoto Encyclopedia of Genes and Genomes (KEGG)[45] enrichment analysis and $p\text{adj} < 0.05$ was used as the threshold for significant enrichment. Protein-protein interaction (PPI) analysis was performed based on the interactions in the STRING protein interaction database. Analysis and hub gene screening was performed by the MCODE plug-in of Cytoscape software.

RT-qPCR

RT-qPCR was used to validate the reliability of the sequencing outcomes. β-actin was selected as the internal reference gene. Total RNA was extracted with TRIzol reagent (15596026, Lifetech, China). Following this, RNA was converted into cDNA utilizing the FastKing RT cDNA (With gDNase) kit (KR116, Tiangen, China), adhering to the manufacturer's guidelines. cDNA was extracted with Taq Pro Universal SYBR qPCR Master Mix (Q712-02, Vazyme, China) to amplify the target gene and perform real-time RT-PCR for quantification. The instrument used for RT-qPCR was the 7500 Real-Time PCR System (Applied Biosystems, USA). PCR cycling conditions were as follows: 95 °C for 10 min; 95 °C for 15s; 60 °C for 30s; repeated for 40–45 cycles. The relative expression of the genes was calculated using the $2^{-\Delta\Delta Ct}$ method. Primers used for RT-PCR are shown in Table 2.

Western Blot

To assess changes in hub genes at the translational level, tissue proteins were extracted using RIPA buffer (P0013B, Beyotime, China) containing a protease inhibitor mixture. The lysates underwent separation via 10% SDS-PAGE. Then, the proteins were transferred onto a PVDF membrane. Skimmed milk (5%, pH 7.5) was used to block proteins. Then, proteins were incubated with primary antibodies overnight at 4°C. Incubating the secondary antibody after rinsing the membrane. Lastly, Immobilon Western Chemiluminescent HRP Substrate (WBKLS0100, Millipore, China) was used to

Table 2 List of Primers

Gene	F (5′-3′)	R (5′-3′)
β-actin	CTGGAGAAGAGCTATGAG	GATGGAATTGAATGTAGTTTC
Bgn	CTGAGACCCTGAATGAAC	TTGGAGTAGCGAAGTAGA
Serpine1	ACAAGTCTGATGGTAGCA	GTGGTGAACTCAGTGTAG
Ctsb	AAGGAAGATAAGCACTAT	TAAGTCAAGAAGTCAGAA
Tnfaip6	GTGTGGTGGTGTCTTTAC	TGGTTGTCGTCATACTCA
Lum	AACATTCCTGATGAGTAT	TCATTAACGGTTGGTATA

Note: Italics represent gene names.

develop color. Antibodies: mouse anti-β-actin monoclonal antibody (1:4000, TA-09, Zhongsui Jinqiao, China), Bgn (1:2000, 16409-1-AP, proteintech, China), Serpine1 (1:2000, bs-1704R, Bioss, China), Ctsb (1:2000, bs-1500R, Bioss, China), Tnfaip6 (1:1000, 13321-1-AP, proteintech, China), Lum (1:1000, 10677-1-AP, proteintech, China), Goat Anti Mouse IgG -HRP (1:4000, M21001L, Abmart, Shanghai, China), Goat Anti Rabbit IgG-HRP (1:4000, M21002L, Abmart, Shanghai, China).

Statistical Analysis

Data are expressed as mean ± standard deviation of at least 3 sets of parallel independent experiments. Statistical analysis of variance was assessed using one-way ANOVA and Tukey post hoc tests. Statistical significance was indicated as * $p \leq 0.05$, ** $p \leq 0.01$, *** $p \leq 0.001$. Statistical Product and Service Solutions (SPSS, v 23.0, IBM, USA) for statistical analysis. Origin (v 2021, OriginLab Corporation, USA) for visualization.

Results

Successful Construction of a KOA Model and Initial Investigation of Arthritis in Each Group of Rats After Four weeks of Treatment

After modeling the SD rats, we monitored their body weights over four successive weeks. Moreover, the AI of the rats in each group at week four was evaluated. Our findings indicated a progressive increase in body weights across all groups, with intergroup differences remaining below 10.7 g at that time (Figure 1B). Furthermore, the AI observed in the other three groups significantly surpassed that of the Sham group by week four (week 0 of treatment), confirming the effectiveness of our modeling (Figure 1D). Subsequently, we administered CKA-L to the Treatment group and NSAID piroxicam to the Piroxicam group. Post-treatment results revealed that the weight gain trend in the Sham group exceeded that of the other three groups (Figure 1C). A comparative analysis indicated a decrease in AI for the Treatment group relative to the Model group, although this difference lacked statistical significance. Conversely, the Piroxicam group demonstrated a noteworthy reduction in AI compared to the Model group. Within-group comparisons revealed a significant decrease in AI for the Treatment group by week four, while the Piroxicam group showed significant reductions beginning at week three (Figure 1D). Subsequently, we assessed the osteoarthritic status using Safranin O–Fast Green staining and quantified the changes with the OARSI scoring system.[46] The results showed that the OARSI score was significantly higher in the model group (Figure 1E). These results suggest that both CKA-L and piroxicam treatments effectively lower AI in rats with degenerative KOA, although CKA-L appears to exhibit a slower response than piroxicam.

Both CKA-L and Piroxicam Effectively Treat KOA

After 4 weeks of treatment in SD rats, we utilized X-ray imaging to assess the knee joints across all groups. The findings revealed a significant gap between the femur and tibia in the Model group, characterized by low bone density, absent articular cartilage, and an irregular surface. In contrast, the knee joints of rats receiving CKA-L and piroxicam treatments exhibited a reduced gap, enhanced bone density, and evidence of tissue or cartilage regeneration in areas previously lacking cartilage (Figure 2A). Subsequently, we quantified the levels of IL-1β and TNF-α across the groups. The results

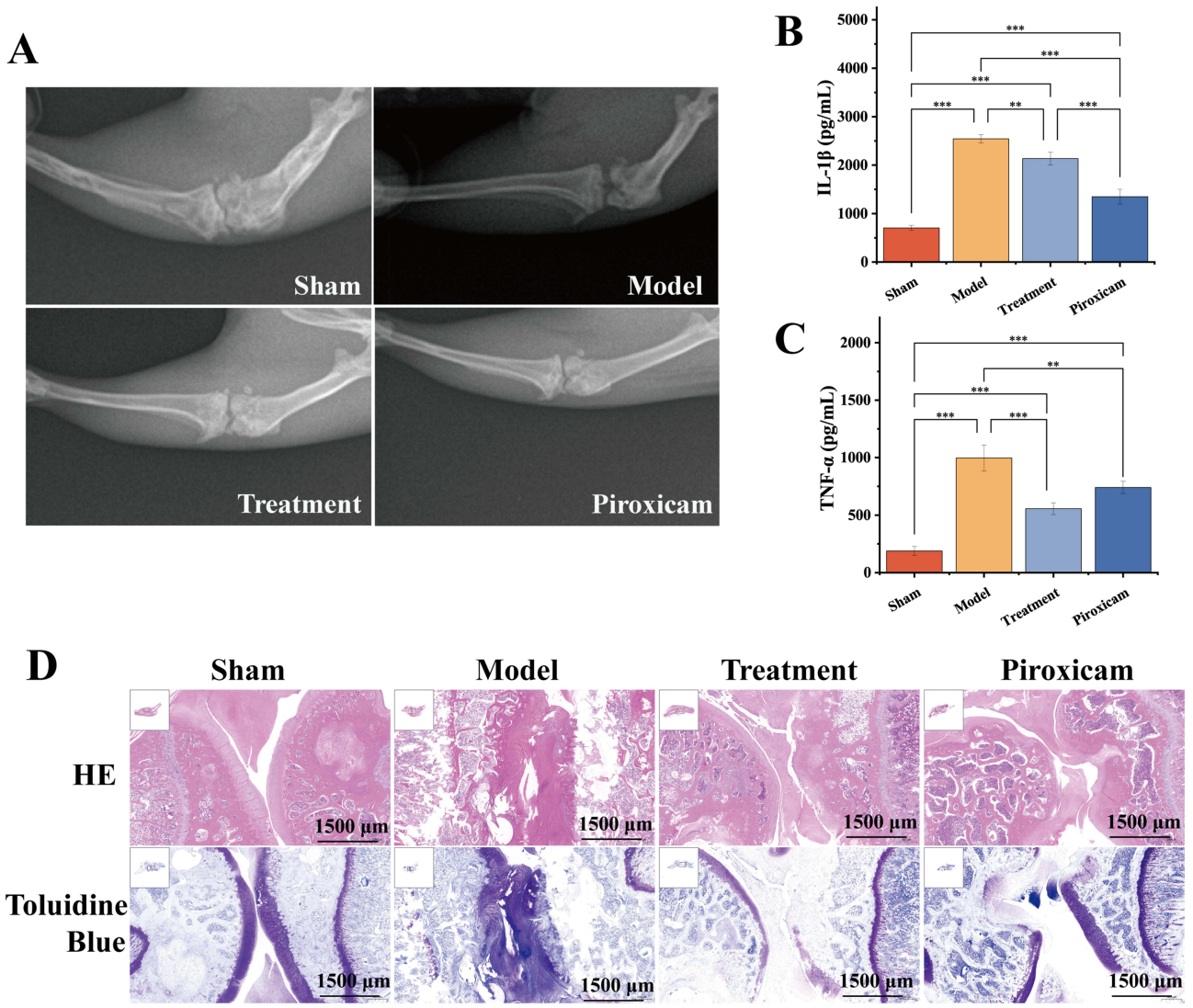

Figure 2 Study of chondrogenesis and cytokines in CKA-L treatment. (**A**) X-ray analysis of knee joint repair. (**B** and **C**) ELISA analysis of IL-1β (**B**) and TNF-α (**C**) contents. (**D**) HE (upsides) and toluidine blue (downside) (cartilage matrix blue-violet or purple) staining to observe the cartilage condition; Scar bar: 2500 μm. Data are expressed as mean ± SD of four parallel independent experiments. Statistical significance was indicated as ** $p \leq 0.01$, *** $p \leq 0.001$.

indicated a marked increase in these inflammatory cytokines in the Model group, which significantly decreased following CKA-L and piroxicam treatment (Figure 2B and C). Notably, TNF-α levels exhibited a more pronounced reduction in the CKA-L treatment group compared to the piroxicam group (p=0.047) (Figure 2C). These findings suggest that CKA-L presents a promising therapeutic option for KOA. Furthermore, we employed staining to evaluate chondrocyte damage. HE and toluidine blue staining revealed intact and smooth cartilage in the Sham group, with chondrocytes evenly distributed. However, the Model group displayed irregular knee joint tissue, decreased chondrocyte counts, disorganized arrangements, and significant articular cartilage loss (Figure 2D). Post-treatment, KOA rats exhibited considerable repair in knee joint integrity, with an increase in chondrocytes organized in a single column (Figure 2D). These results reinforce that both CKA-L and piroxicam serve as effective treatments for KOA.

Gene Expression Analysis and Identification of DEGs

To further investigate the mechanism underlying CKA-L's efficacy in treating KOA, we conducted high-throughput transcriptome sequencing (GSE308025) on 12 samples (comprising Sham, model, and treatment groups, each with four replicates). The transcriptome analysis generated 79.76 G of CleanData, achieving Q30 base scores between 94.54% and

https://doi.org/10.2147/JPR.S547968

95.18%, with an average GC content of 50.72%. The gene expression level distribution across samples is depicted in Figure 3A, indicating sufficient data quality for comprehensive analysis. Principal Component Analysis (PCA) accounted for 71.32% of the variance, demonstrating genetic divergence between the treatment group and the other groups, excluding the model2. On the secondary factor (15.54%), the treatment4 and the Sham group samples clustered in the upper half of the plot, while the remaining samples fell in the lower half (Figure 3B). Furthermore, we identified 3363 DEGs in the Treatment vs Model group, with 1108 up-regulated and 2255 down-regulated (Figure 3C). The Treatment vs Sham group identified 5704 DEGs, 2886 up-regulated and 2818 down-regulated (Figure 3D). The Model vs Sham group identified 422 DEGs, 175 up-regulated and 247 down-regulated (Figure 3E).

GO and KEGG Enrichment Analysis of DEGs

Subsequently, the DEGs were further analyzed for GO and KEGG enrichment. The GO enrichment results were categorized into three components: biological process (BP), cellular component (CC), and molecular function (MF). For each group, we selected the top ten most significant entries in each category for visualization. In the BP category, both Model vs Sham and Treatment vs Model groups exhibited varying degrees of enrichment in DNA metabolic process

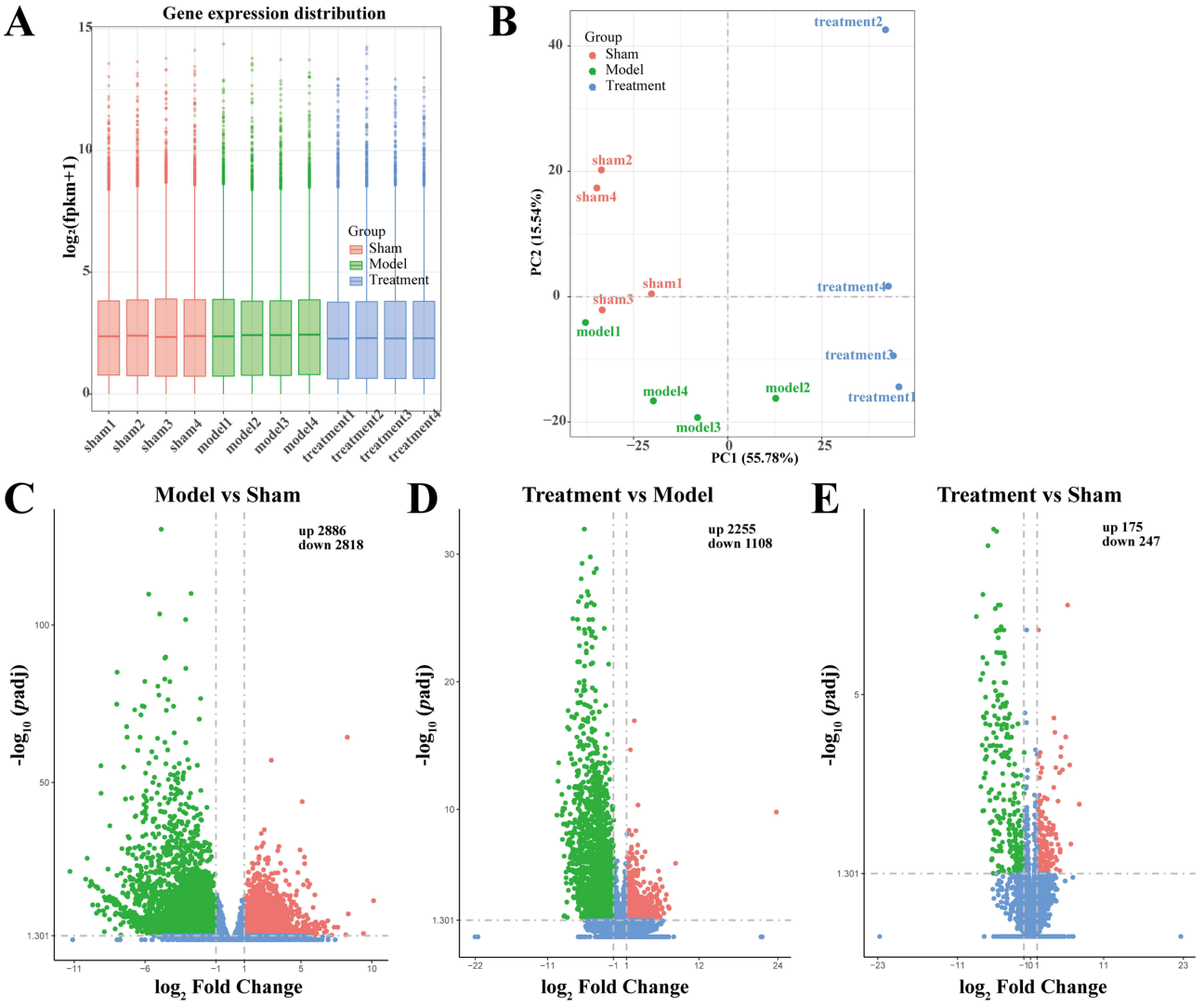

Figure 3 Gene expression levels and differential gene analysis of CKA-L treatment. (**A**) Analysis of gene expression levels of FPKM box line plot. (**B**) Principal Component Analysis plot. (**C**–**E**) DEGs volcano plots of Model vs Sham group (**C**), Treatment vs Model group (**D**), and Treatment vs Sham group (**E**) (genes with non-significant differences in blue, significantly up-regulated differential genes in red and significantly down-regulated differential genes in green).

(GO:0006259), DNA replication related process (GO:0006260, GO:0006270, GO:0006261), and movement of cell or subcellular component (GO:0006928) (Figure 4A). Additionally, the Treatment vs Model group showed enrichment in terms related to chromosome organization (GO:0051276), microtubule-based movement and process (GO:0007018 and 0007017), response to stress (GO:0006950), and system development (GO:0048731) (Figure 4A). Regarding CC, DEGs in both Model vs Sham and Treatment vs Model groups were differentially enriched in terms such as chromosomal part (GO:0044427), chromosome (GO:0005694), chromosome, centromeric region (GO:0000775), DNA packaging complex (GO:0044815), kinetochore (GO:0000776), nucleosome (GO:0000786), and protein-DNA complex (GO:0032993) (Figure 4B). Moreover, DEGs in the Treatment vs Model and Treatment vs Sham groups were enriched in the extracellular region (GO:0005576), while the Model vs Sham group had greater enrichment in the extracellular matrix (GO: 0031012) (Figure 4B). In the MF category, DEGs in both Model vs Sham and Treatment vs Model groups were enriched in cysteine-type endopeptidase inhibitor activity (GO:0004869) and motor activity (GO:0003774) (Figure 4C). Additionally, DEGs in both Treatment vs Model and Treatment vs Sham groups were enriched in calcium ion binding (GO:0005509) term (Figure 4C).

For KEGG enrichment analysis, we created a bubble map to illustrate the top 20 signaling pathways enriched by DEGs across the three comparison groups (Figure 4D–F). Notably, nine pathways were common among the top 20 for both Model vs Sham and Treatment vs Model groups. These pathways included Cell cycle (rno04110), Complement and coagulation cascades (rno04610), DNA replication (rno03030), ECM-receptor interaction (rno04512), Hematopoietic cell lineage (rno04640), Malaria (rno05144), Protein digestion and absorption (rno04974), Systemic lupus erythematosus (rno05322) and Viral protein interaction with cytokine and cytokine receptor (rno04061). Moreover, the Model vs Sham and Treatment vs Sham groups were both enriched in the Hypertrophic cardiomyopathy pathway (rno05410).

The enrichment analysis of DEGs in the Treatment vs Model group, combined with prior analyses, revealed significant findings. In BP, the terms related to DNA metabolic process, DNA replication, DNA-dependent DNA replication, and DNA replication initiation terms were up-regulated. In CC, terms such as chromosome, chromosomal part, chromosome, centromeric region, kinetochore, DNA packaging complex, nucleosome, and protein-DNA complex also showed up-regulated. In MF, terms indicating cysteine-type endopeptidase inhibitor activity were up-regulated, while motor activity terms decreased (Figure 5A and B). The KEGG enrichment analysis indicated that pathways related to the Cell cycle, DNA replication, Hematopoietic cell lineage, and Systemic lupus erythematosus pathways were up-regulated. Conversely, Malaria, ECM-receptor interaction, Complement and coagulation cascades, Protein digestion and absorption, and Viral protein interaction with cytokine and cytokine receptor pathways were down-regulated (Figure 5C and D).

PPI Analysis and Identification, Validation of Hub Genes

To identify hub genes for CKA-L treatment, we performed a PPI analysis on the proteins encoded by DEGs across the three groups. The interaction network revealed a strong correlation among the proteins Serpine1, Bgn, Mmp12, Tnfaip6, Cdkn2, Lum, and Ctsb (Figure 6A). Two Cluster were obtained by Cytoscape's MCODE plug-in. Cluster 1 comprised proteins from 9 genes and achieved a score of 5.25 (Figure 6B). Cluster 2 included proteins from 6 genes with a score of 4 (Figure 6C). After comprehensive screening, five hub genes stood out: *Bgn, Ctsb, Lum, Serpine1*, and *Tnfaip6*. Subsequently, RT-qPCR was used to further evaluate the mRNA expression of these hub genes. The RT-qPCR indicated that all five hub genes exhibited elevated expression in the Model group relative to the Sham group. Post CKA-L treatment, except for *Bgn*, the mRNAs from the other four hub genes demonstrated reduced expression (Figure 6D–H). These findings aligned with high-throughput sequencing results, confirming the reliability of our transcriptome data. We then employed Western blot analysis to corroborate the protein expression of these genes. The results showed that the protein expression and mRNA expression levels of the five hub genes were consistent (Figure 6I–N).

Discussion

Degenerative KOA represents a prevalent chronic condition. While it is non-lethal, the pain and physical limitations it causes significantly hinder daily living.[47] Currently, available treatments have significant side effects or cannot be used in the long term. Moreover, it is crucial to acknowledge the substantial financial burden associated with KOA management. CKA-L emerges as a significant therapeutic approach within TCM, with evidence indicating its cost-effectiveness, which

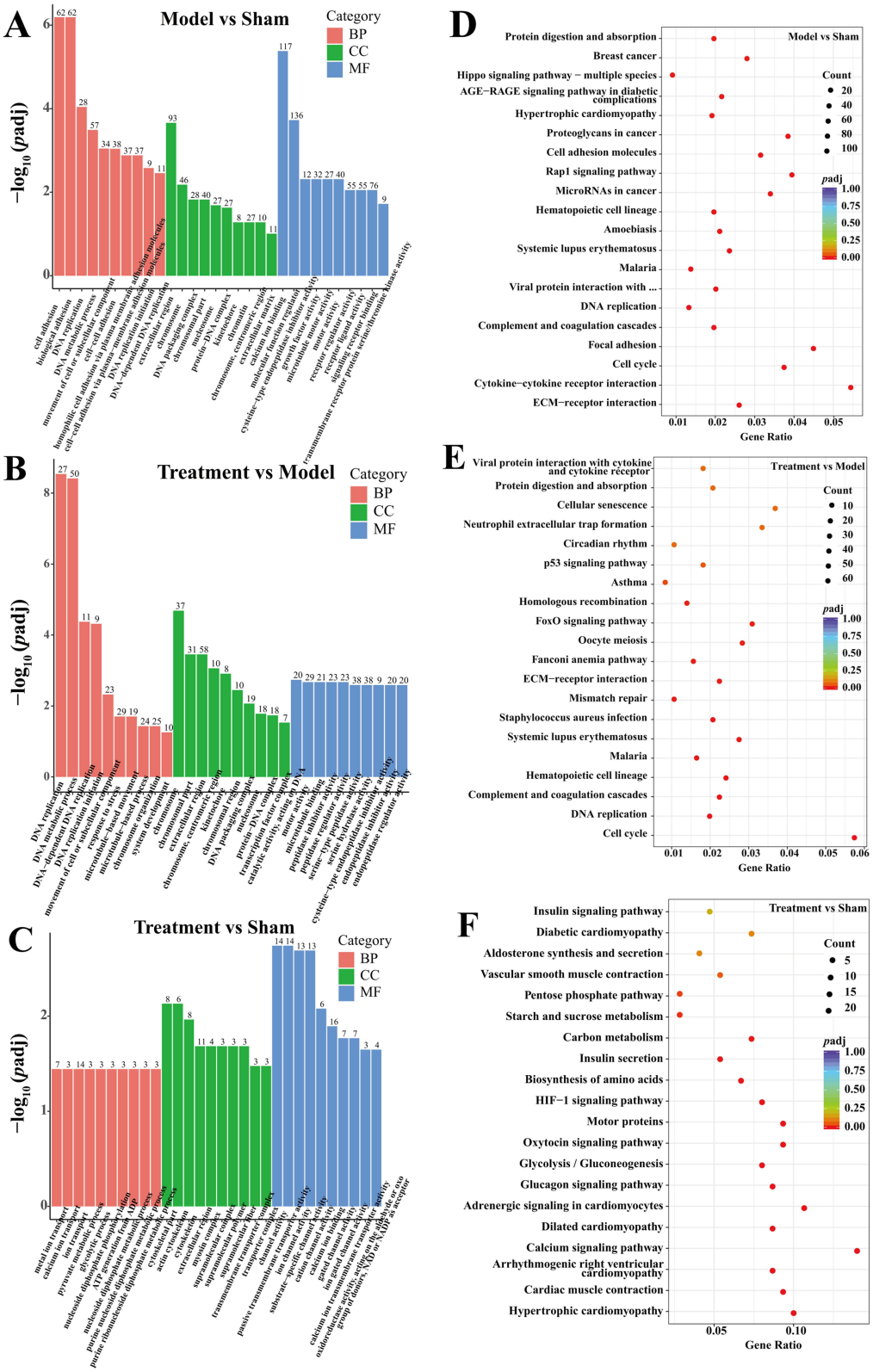

Figure 4 GO and KEGG enrichment analysis of differential genes. (**A**–**C**) GO enrichment analysis of DEGs in Model vs Sham (**A**), Treatment vs Model (**B**), and Treatment vs Sham (**C**) groups. (**D**–**F**) KEGG enrichment analysis of DEGs in Model vs Sham (**D**), Treatment vs Model (**E**), and Treatment vs Sham (**F**) groups.

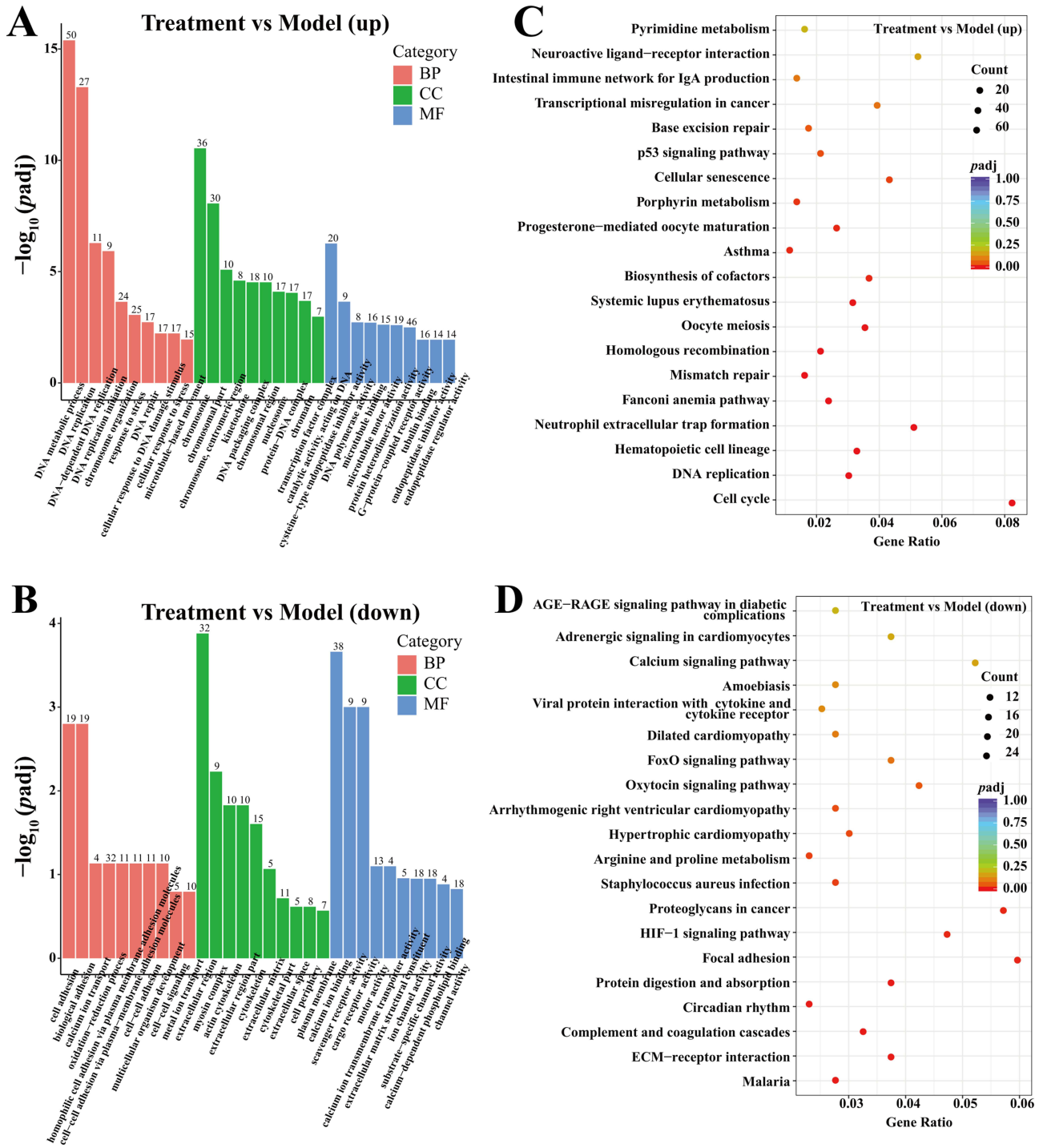

Figure 5 GO and KEGG enrichment analysis of DEGs in Treatment vs Model group. (**A** and **B**) GO enrichment analysis of up-regulated (**A**) and down-regulated (**B**) DEGs in the Treatment vs Model group. (**C** and **D**) KEGG enrichment analysis of up-regulated (**C**) and down-regulated (**D**) DEGs in the Treatment vs Model group.

greatly enhances the superiority of CKA-L as a treatment for KOA.[23,24] Piroxicam is an effective therapeutic drug for KOA.[13] Our investigation revealed that although the AI of piroxicam was significantly lower than that of CKA-L in the early stages, after a 4-week treatment period, the AI of both CKA-L and piroxicam decreased significantly. Moreover, analyses via X-ray, HE, and toluidine blue staining confirmed that both CKA-L and piroxicam effectively promote chondrocyte regeneration. These results suggest that CKA-L treatment, although slower than piroxicam, is an effective treatment for KOA. Additionally, existing literature suggests that CKA-L has minimal side effects (the main symptoms

https://doi.org/10.2147/JPR.S547968

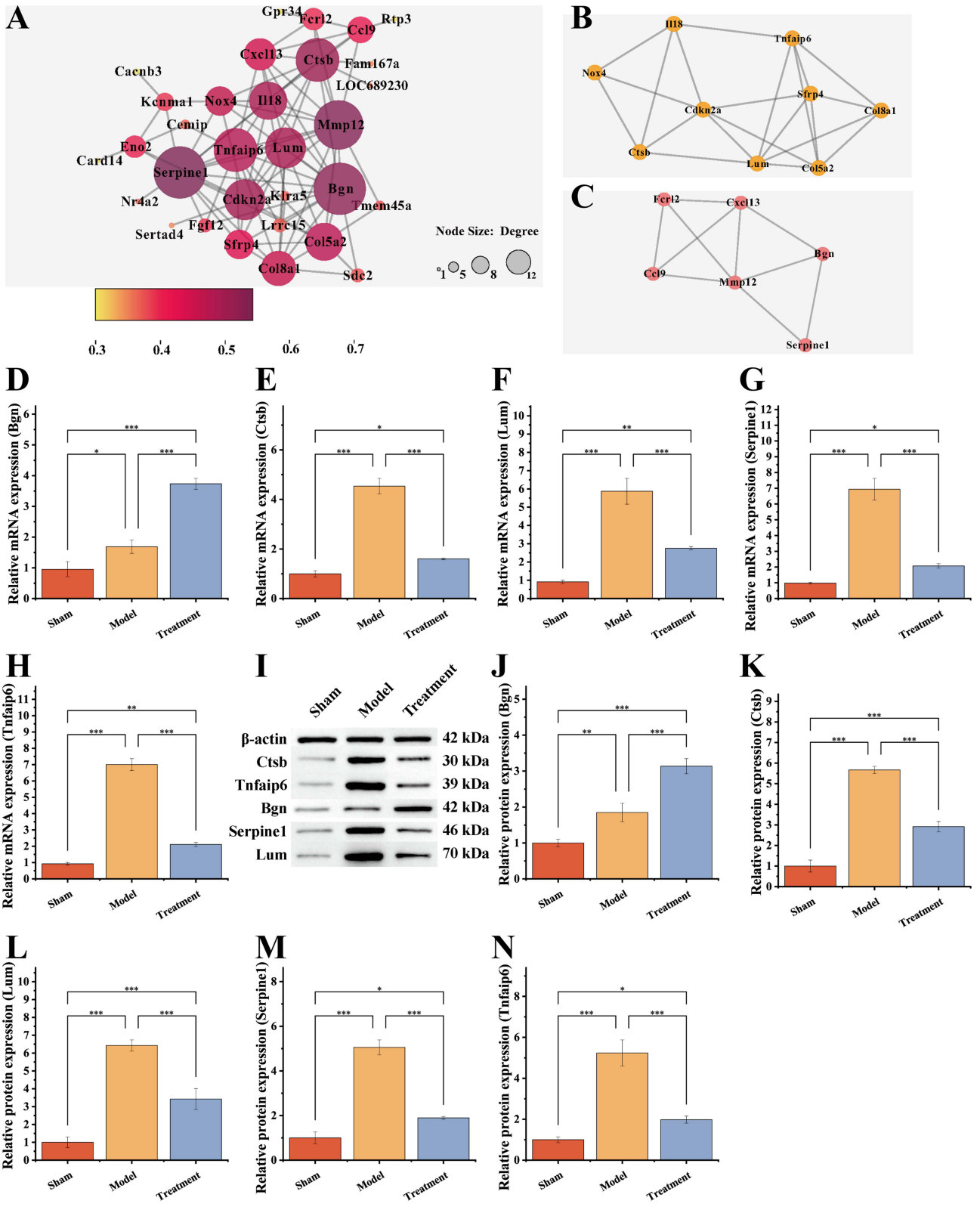

Figure 6 Protein interactions analysis and validation of hub genes. (**A**–**C**) General diagram of protein interactions analysis encoded by three groups of DEGs (**A**), Cluster 1 (**B**), and Cluster 2 (**C**) obtained according to the MCODE algorithm. (**D**–**H**) RT-qPCR was used to analyze the mRNA expression levels of hub genes Bgn (**D**), Ctsb (**E**), Lum (**F**), Serpine1 (**G**), and Tnfaip6 (**H**). (**I**–**N**) Western blot (**I**) was used to verify the protein expression levels of hub genes Bgn (**J**), Ctsb (**K**), Lum (**L**), Serpine1 (**M**), and Tnfaip6 (**N**). Statistical significance was indicated as * $p \leq 0.05$, ** $p \leq 0.01$, *** $p \leq 0.001$.

are local bleeding, ecchymosis and transient pain),[27,48,49] highlighting its potential as a favorable economic and prognostic solution for KOA treatment. Furthermore, inflammation plays a pivotal role in the onset and progression of KOA.[50] Among the pro-inflammatory cytokines, TNF-α and IL-1β stand out as significant contributors to the disease process.[51] In this study, we demonstrated that CKA-L effectively reduced the levels of these cytokines, aligning with findings from previous research.[52] Notably, the results in this study indicated that the Treatment group exceeded the Piroxicam group in reducing TNF-α levels. Previous studies have extensively used acupuncture for the treatment of KOA, yielding favorable outcomes.[28–30] However, these studies often involved a large selection of acupoints, typically choosing 6 to 8 from a pool of over a dozen, or employing between 8 to more than 10 different acupoints for treatment.[28,31–33] In contrast, the CKA-L approach selects only the Weizhong, Heding, and inner and outer Xiyan acupoints for intervention, demonstrating notable efficacy. This strategy highlights advantages such as fewer selected points, ease of application, and significant therapeutic results.

Afterward, to further elucidate the underlying mechanisms of CKA-L's action on KOA, we conducted high-throughput transcriptome sequencing analysis on the Sham, Model, and Treatment groups. The results showed that DEGs in the Treatment group were enriched in the extracellular region whereas those in the Model group were more enriched in the extracellular matrix. This finding implies that the extracellular matrix may be critical to CKA-L's positive therapeutic effects on KOA. Further analyzed in the Treatment vs Model group from the up-regulated and down-regulated DGEs. The results of GO enrichment analysis found that the DNA metabolic process, DNA replication, and the entry cysteine-type endopeptidase inhibitor activity terms were up-regulated. From the results of KEGG enrichment analysis, the Cell cycle and DNA replication pathways were up-regulated. Studies strong associations between DNA damage repair mechanisms[53] and chondrocyte senescence[54] in the progression of KOA. Our findings align with this, revealing that DEGs cluster within pathways related to DNA repair and the cell cycle. Furthermore, we observed that these DEGs exhibit significant enrichment in molecular pathways inhibiting cysteine-type endopeptidases, which are linked to chondrocyte apoptosis.[55–57] These results suggest that CKA-L may facilitate KOA treatment by enhancing DNA repair, restraining cysteine-type endopeptidases, and promoting cell cycle dynamics to stimulate chondrocyte regeneration. Subsequent PPI analysis identified five hub genes including *Bgn, Ctsb, Lum, Serpine1*, and *Tnfaip6. Bgn* (Biglycan) encodes a protein-rich glycoprotein macromolecular complex.[58] Notably, *Bgn* promotes osteoblast differentiation through TLR3-dependent signaling[59] and serves as a key factor in myocyte differentiation and skeletal muscle regeneration.[60] Reduced sequestration of *Bgn* in the extracellular matrix promotes chondrogenesis via TGF-β1.[61] *Ctsb* (Cathepsin B) is a lysosomal cysteine protease whose primary functions are associated with immunity and inflammation.[62] Moreover, *Ctsb* participates in IL-1β-induced chondrocyte damage.[63] *Lum* (Lumican) is a small-molecule proteoglycan rich in leucine. Research indicates that Lum participates in TLR4-induced cartilage degradation and proinflammatory activation.[64] *Serpine1* (Serpin Family E Member 1), encoding plasminogen activator inhibitor-1 (PAI-1), primarily participates in regulating the coagulation-fibrinolysis balance, extracellular matrix (ECM) degradation, and inflammatory responses.[65] Furthermore, *Serpine1* is associated with cartilage destruction.[66,67] *Tnfaip6* (TNF-α induced protein 6) encodes TSG-6, belongs to the hyaluronan-binding protein family and participates in the stabilization and remodeling of the ECM.[68] Besides, *Tnfaip6* impairs the assembly of hyaluronan aggregation proteins.[68,69] These studies indicate that *Ctsb, Lum, Serpine1*, and *Tnfaip6* are associated with inflammation and inflammation-induced bone injury and inhibition of bone healing. Conversely, *Bgn* is linked to bone and muscle repair and regeneration. This effectively explains the reduction in mRNA and protein expression of the four pivotal genes—excluding *Bgn*—following CKA-L treatment. CKA-L may suppress inflammation and bone damage by downregulating *Ctsb, Lum, Serpine1*, and *Tnfaip6*, while promoting repair and regeneration of knee cartilage and muscle by upregulating *Bgn*.

In summary, our study illustrates that CKA-L is a promising therapeutic approach for KOA, potentially through mechanisms such as enhanced DNA repair, cell cycle promotion, and cysteine-type endopeptidase inhibition, aiding chondrocyte regeneration. It is essential to recognize that our mechanism analyses stem from bioinformatics evaluations, necessitating further empirical investigations. Furthermore, it is important to note that the sample size in this study is small, necessitating further research and validation with larger cohorts. Although our study is based on a mouse model, it is essential to conduct mechanism studies in cell models and explore additional clinical applications. Additional research to clarify the mechanism of CKA-L will help integrate it with complementary approaches such as dietary therapy, thereby

enhancing its therapeutic efficacy. Nonetheless, these findings provide valuable theoretical insights that support the application of CKA-L as a cost-effective and low-risk treatment for KOA.

Conclusion

This study confirms CKA-L as an effective intervention for degenerative KOA, based on AI assessments, X-ray imaging, histological evaluations, and pro-inflammatory cytokine quantification. Transcriptomic analysis reinforces CKA-L's positive role in KOA management by promoting DNA repair, inhibiting cysteine-type endopeptidases, and fostering chondrocyte growth through cell cycle enhancement. Additionally, five hub genes, *Bgn, Ctsb, Lum, Serpine1*, and *Tnfaip6*, were identified. The findings in this study provide an effective, low-cost, low-risk treatment pathway for KOA. Meanwhile, this study provides theoretical support for the treatment of KOA with CKA-L.

Data Sharing Statement

Data will be made available on request. The datasets generated and/or analysed in this study are available in NCBI, accession number is GSE308025.

Ethical Declaration

This study was approved by the Experimental Animal Ethics Committee of Yunnan Provincial Hospital of Traditional Chinese Medicine (DSL-2024-048) and strictly adhered to the relevant provisions of the "Guidelines for Ethical Review of Laboratory Animal Welfare" (GB/T 35892-2018), ensuring the welfare of experimental animals was fully safeguarded.

Funding

This study was supported by Joint Yunnan University of Traditional Chinese Medicine Fund projects (grant No. XYLH202348).

Disclosure

The authors report no conflicts of interest in this work.

References

1. Glyn-Jones S, Palmer AJR, Agricola R, et al. Osteoarthritis. *Lancet*. 2015;386:376–387. doi:10.1016/S0140-6736(14)60802-3
2. Pettenuzzo S, Berardo A, Belluzzi E, et al. Mechanical insights into fat pads: a comparative study of infrapatellar and suprapatellar fat pads in osteoarthritis. *Connect Tissue Res*. 2025;66:272–283. doi:10.1080/03008207.2025.2502591
3. Tang C-H. Research of pathogenesis and novel therapeutics in arthritis 3.0. *Int J Mol Sci*. 2023;24:10166. doi:10.3390/ijms241210166
4. Steinmetz JD, Culbreth GT, Haile LM, et al. Global, regional, and national burden of osteoarthritis, 1990–2020 and projections to 2050: a systematic analysis for the Global Burden of Disease Study 2021. *Lancet Rheumatol*. 2023;5:e508–e522. doi:10.1016/S2665-9913(23)00163-7
5. Iorio R, Healy WL. Unicompartmental arthritis of the knee. *J Bone Jt Surg*. 2003;85:1351–1364. doi:10.2106/00004623-200307000-00025
6. Felson DT, Naimark A, Anderson J, et al. The prevalence of knee osteoarthritis in the elderly. The framingham osteoarthritis study. *Arthritis Rheum*. 1987;30:914–918. doi:10.1002/art.1780300811
7. Belluzzi E, El Hadi H, Granzotto M, et al. Systemic and local adipose tissue in knee osteoarthritis. *J Cell Physiol*. 2017;232:1971–1978. doi:10.1002/jcp.25716
8. Segal NA, Nilges JM, Oo WM. Sex differences in osteoarthritis prevalence, pain perception, physical function and therapeutics. *Osteoarthr Cartil*. 2024;32:1045–1053. doi:10.1016/j.joca.2024.04.002
9. Grazina R, Andrade R, Bastos R, et al. Clinical management in early OA. *Adv Exp Med Biol*. 2018;1059:111–135.
10. Felson DT, Zhang Y, Anthony JM, et al. Weight loss reduces the risk for symptomatic knee osteoarthritis in women. *Ann Intern Med*. 1992;116:535–539. doi:10.7326/0003-4819-116-7-535
11. Cole BJ, Harner CD. Degenerative arthritis of the knee in active patients: evaluation and management. *J Am Acad Orthop Surg*. 1999;7:389–402. doi:10.5435/00124635-199911000-00005
12. Knoop J, Dekker J, van der Leeden M, et al. Knee joint stabilization therapy in patients with osteoarthritis of the knee: a randomized, controlled trial. *Osteoarthr Cartil*. 2013;21:1025–1034. doi:10.1016/j.joca.2013.05.012
13. Farpour HR, Estakhri F, Zakeri M, et al. Efficacy of piroxicam mesotherapy in treatment of knee osteoarthritis: a randomized clinical trial. *Evid Based Complement Altern Med*. 2020;2020. doi:10.1155/2020/6940741
14. Grässel S, Muschter D. Recent advances in the treatment of osteoarthritis. *F1000Research*. 2020;9:325. doi:10.12688/f1000research.22115.1
15. Lane JM. Anti-inflammatory medications: selective COX-2 inhibitors. *J Am Acad Orthop Surg*. 2002;10:75–78. doi:10.5435/00124635-200203000-00001
16. Hochberg MC, Altman RD, Brandt KD, et al. Guidelines for the medical management of osteoarthritis. *Arthritis Rheum*. 1995;38:1541–1546. doi:10.1002/art.1780381104

17. Miller EH. Viscosupplementation: therapeutic mechanisms and clinical potential in osteoarthritis of the knee. *J Am Acad Orthop Surg*. 2001;9:146–147.
18. Sonesson S, Springer I, Yakob J, et al. Knee arthroscopic surgery in middle-aged patients with meniscal symptoms: a 10-year follow-up of a prospective, randomized controlled trial. *Am J Sports Med*. 2024;52:2250–2259. doi:10.1177/03635465241255653
19. Hu X, Zhang Z, Zhang W, et al. Efficacy and safety of micro-fragmented adipose tissue combined with knee arthroscopy in the treatment of knee osteoarthritis: a systematic review. *J Orthop Surg Res*. 2025;20:646. doi:10.1186/s13018-025-06006-5
20. Zhang Z, Hu Z, Zhao D, et al. Arthroscopic surgery is not superior to conservative treatment in knee osteoarthritis: a systematic review and meta-analysis of randomized controlled trails. *BMC Musculoskelet Disord*. 2024;25:712. doi:10.1186/s12891-024-07813-3
21. Rönn K, Reischl N, Gautier E, et al. Current surgical treatment of knee osteoarthritis. *Arthritis*. 2011;2011:454873. doi:10.1155/2011/454873
22. Losina E, Paltiel AD, Weinstein AM, et al. Lifetime medical costs of knee osteoarthritis management in the United States: impact of extending indications for total knee arthroplasty. *Arthritis Care Res*. 2015;67:203–215. doi:10.1002/acr.22412
23. Zhao J, Shi X. Investigation and analysis of the present situation of acupuncturist in China. *China Med Her*. 2011;8(18):152–153.
24. Wang H, Gusmano MK, Cao Q. An evaluation of the policy on community health organizations in China: will the priority of new healthcare reform in China be a success? *Health Policy*. 2011;99:37–43. doi:10.1016/j.healthpol.2010.07.003
25. Yang M, Jiang L, Wang Q, et al. Traditional Chinese medicine for knee osteoarthritis: an overview of systematic review. *PLoS One*. 2017;12:e0189884. doi:10.1371/journal.pone.0189884
26. Van Hal M, Dydyk AM, Green MS. *Acupuncture*. Treasure Island (FL): StatPearls Publishing; 2025.
27. Liu WH, Chen C, Wang F, et al. Development trend and current situation of acupuncture-moxibustion indications. *World J Acupunct Moxibustion*. 2020;30:245–250. doi:10.1016/j.wjam.2020.07.014
28. Selfe TK, Taylor AG. Acupuncture and Osteoarthritis of the Knee. *Fam Community Health*. 2008;31:247–254. doi:10.1097/01.FCH.0000324482.78577.0f
29. Manheimer E, Linde K, Lao L, et al. Meta-analysis: acupuncture for osteoarthritis of the knee. *Ann Intern Med*. 2007;146:868–877. doi:10.7326/0003-4819-146-12-200706190-00008
30. Ezzo J, Hadhazy V, Birch S, et al. Acupuncture for osteoarthritis of the knee: a systematic review. *Arthritis Rheum*. 2001;44:819–825. doi:10.1002/1529-0131(200104)44:4<819::AID-ANR138>3.0.CO;2-P
31. Trial ATR, Scharf H, Mansmann U, et al. Annals of internal medicine article acupuncture and knee osteoarthritis. *Ann Intern Med*. 2013;145:1–16.
32. Witt C, Brinkhaus B, Jena S, et al. Acupuncture in patients with osteoarthritis of the knee: a randomised trial. *Lancet*. 2005;366:136–143. doi:10.1016/S0140-6736(05)66871-7
33. Shichao Yu JZ. Exploring the rule of selecting acupoints for acupuncture and moxibustion in the treatment of knee osteoarthritis based on literature analysis. *Chin Med Mod Distance Educ China*. 2023;21:39–41.
34. Wang Y. Observation on the efficacy of Guan's six spirit points for knee pain in the treatment of 38 cases of osteoarthritis of the knee. *J Yunnan Univ Chinese Med*. 2000;23:45–46.
35. Guanglian Xiao SD. Effect of warming needle moxibustion and electroacupuncture on knee function and quality of life of patients with degenerative knee arthritis. *Chin Med Mod Distance Educ China*. 2024;22:111–113.
36. Vas J, Méndez C, Perea-Milla E, et al. Acupuncture as a complementary therapy to the pharmacological treatment of osteoarthritis of the knee: randomised controlled trial. *Br Med J*. 2004;329:1216–1219. doi:10.1136/bmj.38238.601447.3A
37. Berman BM, Lao L, Langenberg P, et al. Effectiveness of acupuncture as adjunctive therapy in osteoarthritis of the knee. *Ann Intern Med*. 2004;141:901. doi:10.7326/0003-4819-141-12-200412210-00006
38. Deng X, Huang L, Li J, et al. Observation on the therapeutic effect of Yi-Ping Lin circum-knee acupuncture based on the three-discrimination theory in treating knee osteoarthritis pain. *Inner Mong J Tradit Chin Med*. 2024;43:10.
39. Galois L, Etienne S, Grossin L, et al. Dose–response relationship for exercise on severity of experimental osteoarthritis in rats: a pilot study. *Osteoarthr Cartil*. 2004;12:779–786. doi:10.1016/j.joca.2004.06.008
40. Cheng M, Zhang X, Shang P, Pu G. An overview of the study of acupoint localization in experimental rats and mice. *Shanghai J Acupunct Moxibustion*. 2021;40:640–646.
41. Dai M, Wei W, Shen Y-X, et al. Glucosides of Chaenomeles speciosa remit rat adjuvant arthritis by inhibiting synoviocyte activities. *Acta Pharmacol Sin*. 2003;24:1161–1166.
42. Smolinska V, Klimova D, Danisovic L, et al. Synovial fluid markers and extracellular vesicles in rheumatoid arthritis. *Medicina*. 2024;60:1945. doi:10.3390/medicina60121945
43. Love MI, Huber W, Anders S. Moderated estimation of fold change and dispersion for RNA-seq data with DESeq2. *Genome Biol*. 2014;15. doi:10.1186/s13059-014-0550-8
44. Gene Ontology Consortium. The gene ontology resource: 20 years and still GOing strong. *Nucleic Acids Res*. 2018;47:D330–D338.
45. Kanehisa M. KEGG: kyoto encyclopedia of genes and genomes. *Nucleic Acids Res*. 2000;28:27–30. doi:10.1093/nar/28.1.27
46. Pritzker KPH, Gay S, Jimenez SA, et al. Osteoarthritis cartilage histopathology: grading and staging. *Osteoarthr Cartil*. 2006;14:13–29.
47. Ettinger WHJ, Afable RF. Physical disability from knee osteoarthritis: the role of exercise as an intervention. *Med Sci Sports Exerc*. 1994;26:1435–1440. doi:10.1249/00005768-199412000-00004
48. Lin JG, Chen YH. The mechanistic studies of acupuncture and moxibustion in Taiwan. *Chin J Integr Med*. 2011;17:177–186. doi:10.1007/s11655-011-0664-8
49. Bäumler P, Zhang W, Stübinger T, et al. Acupuncture-related adverse events: systematic review and meta-analyses of prospective clinical studies. *BMJ Open*. 2021;11:e045961. doi:10.1136/bmjopen-2020-045961
50. Sharma L. Osteoarthritis of the Knee. *N Engl J Med*. 2021;384:51–59. doi:10.1056/NEJMcp1903768
51. Fernandes JC, Martel-Pelletier J, Pelletier J-P. The role of cytokines in osteoarthritis pathophysiology. *Biorheology*. 2002;39:237–246.
52. Shi GX, Tu JF, Wang TQ, et al. Effect of electro-acupuncture (EA) and manual acupuncture (MA) on markers of inflammation in knee osteoarthritis. *J Pain Res*. 2020;13:2171–2179. doi:10.2147/JPR.S256950
53. Neri S, Guidotti S, Bini C, et al. Oxidative stress-induced DNA damage and repair in primary human osteoarthritis chondrocytes: focus on IKKα and the DNA mismatch repair system. *Free Radic Biol Med*. 2021;166:212–225. doi:10.1016/j.freeradbiomed.2021.02.020
54. Loeser RF. Aging and osteoarthritis: the role of chondrocyte senescence and aging changes in the cartilage matrix. *Osteoarthr Cartil*. 2009;17:971–979. doi:10.1016/j.joca.2009.03.002

55. Xu HH, Li SM, Xu R, et al. Predication of the underlying mechanism of Bushenhuoxue formula acting on knee osteoarthritis via network pharmacology-based analyses combined with experimental validation. *J Ethnopharmacol*. 2020;263:113217. doi:10.1016/j.jep.2020.113217
56. Wu L, Chen Y, Chen M, et al. Application of network pharmacology and molecular docking to elucidate the potential mechanism of Astragalus–Scorpion against prostate cancer. *Andrologia*. 2021;53:1–18. doi:10.1111/and.14165
57. Li C, Zheng Z. Cartilage targets of knee osteoarthritis shared by both genders. *Int J Mol Sci*. 2021;22:1–25.
58. Meester JAN, De Kinderen P, Verstraeten A, et al. Meester-loeys syndrome. *Adv Exp Med Biol*. 2021;1348:265–272.
59. Gollmann-Tepeköylü C, Graber M, Hirsch J, et al. Toll-like receptor 3 mediates aortic stenosis through a conserved mechanism of calcification. *Circulation*. 2023;147:1518–1533. doi:10.1161/CIRCULATIONAHA.122.063481
60. Zhang X, He L, Wang L, et al. CLIC5 promotes myoblast differentiation and skeletal muscle regeneration via the BGN-mediated canonical Wnt/β-catenin signaling pathway. *Sci Adv*. 2024;10:eadq6795. doi:10.1126/sciadv.adq6795
61. Embree MC, Kilts TM, Ono M, et al. Biglycan and fibromodulin have essential roles in regulating chondrogenesis and extracellular matrix turnover in temporomandibular joint osteoarthritis. *Am J Pathol*. 2010;176:812–826. doi:10.2353/ajpath.2010.090450
62. Ma K, Chen X, Liu W, et al. CTSB is a negative prognostic biomarker and therapeutic target associated with immune cells infiltration and immunosuppression in gliomas. *Sci Rep*. 2022;12:4295. doi:10.1038/s41598-022-08346-2
63. Zhang C, He W. Circ_0020014 mediates CTSB expression and participates in IL-1β-prompted chondrocyte injury via interacting with miR-24-3p. *J Orthop Surg Res*. 2023;18. doi:10.1186/s13018-023-04370-8
64. Barreto G, Senturk B, Colombo L, et al. Lumican is upregulated in osteoarthritis and contributes to TLR4-induced pro-inflammatory activation of cartilage degradation and macrophage polarization. *Osteoarthr Cartil*. 2020;28:92–101. doi:10.1016/j.joca.2019.10.011
65. Yaron JR, Zhang L, Guo Q, et al. Fibrinolytic serine proteases, therapeutic serpins and inflammation: fire dancers and firestorms. *Front Cardiovasc Med*. 2021;8:648947. doi:10.3389/fcvm.2021.648947
66. Wilkinson DJ. Serpins in cartilage and osteoarthritis: what do we know? *Biochem Soc Trans*. 2021;49:1013–1026. doi:10.1042/BST20201231
67. Masuko K. A suppressive effect of prostaglandin E2 on the expression of SERPINE1/plasminogen activator inhibitor-1 in human articular chondrocytes: an in vitro pilot study. *Open Access Rheumatol Res Rev*. 2009;1:9–15.
68. Chou C-H, Attarian DE, Wisniewski H-G, et al. TSG-6–a double-edged sword for osteoarthritis (OA). *Osteoarthr Cartil*. 2018;26:245–254. doi:10.1016/j.joca.2017.10.019
69. Li C, Zheng Z. Identification of novel targets of knee osteoarthritis shared by cartilage and synovial tissue. *Int J Mol Sci*. 2020;21:1–19.